# Symmetrical Quasi-Reflectionless SAW-Based Bandpass Filters With Tunable Bandwidth

Dimitra Psychogiou<sup>®</sup>, Member, IEEE, and Roberto Gómez-García<sup>®</sup>, Senior Member, IEEE

Abstract—Surface acoustic wave (SAW)-based bandpass filters (BPFs) with symmetrical quasi-reflectionless characteristics and continuously tunable bandwidth (BW) are reported. They are based on in-series-cascaded symmetrical quasi-reflectionless acoustic-wave (AW)-lumped-element resonator (AWLR)-based networks whose input and output ports are connected to resistively terminated AWLR-based bandstop filter (BSF) sections. The proposed concept is presented through the coupling routing diagram (CRD) formalism that allows their design using coupledresonator-based synthesis. It is shown that by incorporating variable reactance elements in their BPF sections, continuous-type BW tuning can be realized. In addition, the fractional BW (FBW) of the filter can be designed to be wider than the electromechanical coupling coefficient  $k_t^2$  of its SAW resonators. This allows enhanced-FBW passbands to be obtained. For proof-of-concept validation, two prototypes were designed and measured. They include a single-stage prototype with 1.9:1 continuously tunable BW and a static two-stage with effective quality factor > 6500, FBW of  $1.2k_t^2$ , and return loss >15 dB throughout its passband and stopband ranges.

Index Terms—Acoustic wave (AW) filter,  $k_t^2$  enhancement, microwave filter, reflectionless filter, surface acoustic wave (SAW) filter.

### I. Introduction

ONVENTIONAL acoustic wave (AW) resonator (AWR)-based filters, such as those based on ladder-/lattice-type arrangements of surface-AW (SAW) and bulk-AW (BAW) resonators, are designed to reflect the RF signals within their stopband regions [1]. This is achieved by presenting a high-majorly reactive-input impedance at frequencies at which unwanted interference is present. Despite their effectiveness in discriminating between the desired in-band signals and undesired interference, the reflected signals in their stopband regions may adversely affect the signal-to-noise ratio (SNR) of the front-end receiver [2]. On the other hand, amplifiers become unstable and mixers downconvert a plethora of spurious signals at the intermediate frequency stages.

To suppress multireflections, nonreciprocal components, such as ferrite-based circulators, are typically added in the RF front-end chain. However, their size is prohibitively large. Input-reflectionless or absorptive filters have been recently

Manuscript received February 16, 2019; revised March 28, 2019 and April 26, 2019; accepted May 17, 2019. Date of publication June 11, 2019; date of current version July 3, 2019. This work was supported by the National Science Foundation under Award 1731956. (Corresponding author: Dimitra Psychogiou.)

- D. Psychogiou is with the Department of Electrical, Computer, and Energy Engineering, University of Colorado Boulder, Boulder, CO 80309 USA (e-mail: dimitra.psychogiou@colorado.edu).
- R. Gómez-García is with the Department of Signal Theory and Communications, Polytechnic School, University of Alcalá, 28871 Alcala de Henares, Spain (e-mail: roberto.gomez.garcia@ieee.org).

Color versions of one or more of the figures in this paper are available online at http://ieeexplore.ieee.org.

Digital Object Identifier 10.1109/LMWC.2019.2918413

investigated as a compact solution alternative [3]–[7]. They are based on: 1) resistively terminated duplexer configurations using lumped element (LE) or microstrip resonators [3], [4] or 2) symmetrical LE filter networks that exhibit complementary even-/odd-mode input-reflection characteristics [5], [6]. Whereas the duplexer-based configurations in [3], [4] effectively cancel the signal reflections at the input access, they are not able to perform this functionality at the filter output port. The reflectionless bandpass filters (BPFs) in [5], [6] exhibit symmetrical reflectionless behavior. However, their practical development requires specific component values that depend on the design frequency and bandwidth (BW). As such, they can only be realized with LEs that exhibit low-quality factors and are not suitable for AWR-based BPF developments.

This letter reports on a new class of AWR-based filters in which symmetrical quasi-reflectionless BPF behavior is obtained at both ports. They are based on AW-lumped-element resonators (AWLRs) combined with LEs, as for example the ones in [7], [8]. The aim of this letter is to extend the duplexer-based concept in [7] to a new type of an AWLR-based frequency-selective network that allows for symmetrical quasi-reflectionless behavior at both of the BPF ports and continuous analog BW tuning. A synthesis method using coupling routing diagrams (CRDs) is reported for the first time.

## II. THEORETICAL FOUNDATIONS

The symmetrical quasi-reflectionless AWLR-based BPF is based on in-series-cascaded quasi-reflectionless stages that comprise: 1) one BPF path shaped by one AWLR and three admittance inverters  $M_A$  and  $M_C$  and is directly connected to the source (S) and the load (L) of the overall filter and 2) two bandstop filters (BSFs) that consist of one AWLR each and are connected to the source and load of the BPF section through two admittance inverters  $M_B$ , Fig. 1(a). Each AWLR is shaped by two nonresonating nodes (NRNs) and two resonating nodes  $R_H$  and  $R_L$  that, respectively, represent the series resonant branch-shaped by a motional inductance  $L_M$  and a motional capacitance  $C_M$  as defined in the Butterworth-Van Dyke (BVD) model of AWRs-of the AWR and the resonance of the resonator formed by the parallel capacitance of the AWR and the LEs  $L_R$  and  $C_R$ , as shown in Fig. 1(b).  $L_R$ ,  $C_R$ , and  $C_P$  are selected to resonate at the center frequency of the desired passband which is equal to the series resonant frequency of the AWR. In this manner, a passband shaped by one pole and two symmetrically located transmission zeros (TZs) is obtained as also discussed in [7]. The BPF design is performed as follows. First, the coupling coefficients of the CRD of the AWLR are obtained by fitting its synthesized response to one of the circuit equivalent in Fig. 1(b) [8]. Note that all the AWLRs resonate at the desired BPF center frequency, i.e., at the normalized frequency  $\Omega = 0$ . Afterwards, the

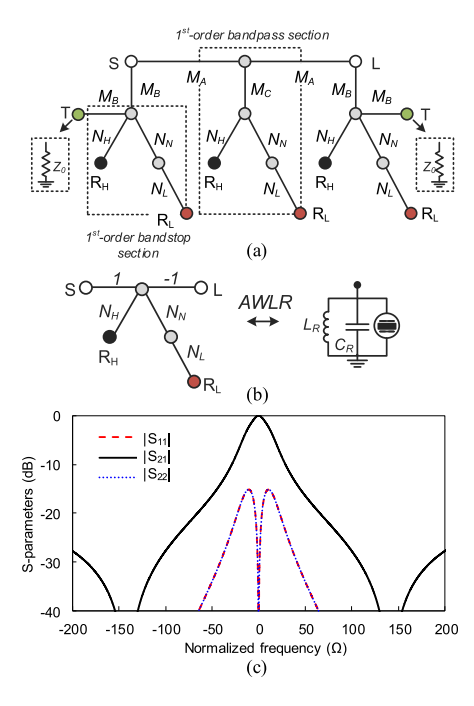


Fig. 1. Symmetrical quasi-reflectionless AWLR-based BPF. (a) CRD (gray circles: zero-susceptance NRNs; white circles: source and load; green circles: resistively terminated NRNs; black circles: high-Q resonant nodes; red circles: low-Q resonant nodes; black lines: couplings; and  $Z_0$ : reference impedance). (b) S-parameters for  $M_A=0.35,\ M_B=1,\ M_C=0.35,\ N_H=1.41$ , and  $N_N=1$ . All resonating nodes and NRNs are defined at  $\Omega=0$ .

symmetrical quasi-reflectionless behavior of the overall BPF shown in Fig. 1(a) is obtained by selecting the admittance inverters so that  $M_C = M_A \cdot M_B$  is satisfied. By altering  $M_B$  (and subsequently  $M_C$ ), the BPF BW can be specified. In addition, the output ports of the BSF sections– NRNs (T) in the CRD in Fig. 1(a) need to be terminated with a resistive load equal to the reference impedance  $Z_0$ . In this manner, the signal energy that is not transmitted by the BPF is absorbed at the resistive nodes.

To demonstrate the operating principles of the symmetrical quasi-reflectionless AWLR-based BPF concept, various synthesized examples are shown in Figs. 1 and 2. In particular, Fig. 1(c) shows the S-parameters of a singlestage quasi-reflectionless AWLR-based BPF which, as can be seen, demonstrates a quasi-inverse-Chebyshev-type BPF response and symmetrical quasi-reflectionless characteristics  $(S_{11} = S_{22})$ . In this example, the CRD of a commercially available SAW resonator–extracted by fitting the RF-measured response of the Abracon ASR418S resonator to the synthesized one by using the methodology in [8]-is used. However, the proposed method is applicable to any two-terminal AWR. By modifying the magnitude of the  $M_B$  inverter, which in turn alters  $M_C$ , the BW of the overall filter can be modified while its two-port quasi-reflectionless behavior is preserved. This is shown in the examples in Fig. 2(a). As it can be seen, lower  $M_B$  values result in wider fractional BWs (FBWs) that can be designed to be significantly broader than the  $0.6k_t^2$  limit of conventional AWR-based ladder and lattice filters, as for example, the ones in [1]. The location of the two TZs of the power transmission response can be also controlled without affecting the two-port quasi-reflectionless behavior. This is achieved by altering the value of the  $N_L$  inverter so that smaller values for  $N_L$  result in passbands with closely-spaced

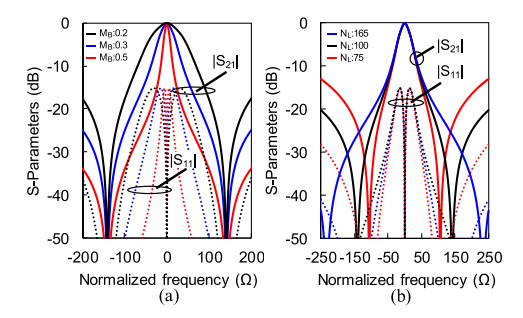


Fig. 2. Synthesized S-parameters for various levels of (a)  $M_B$  and (b)  $N_L$ . The rest of the coupling coefficients are as follows:  $M_B = 0.3$ ,  $M_C = M_A$ .  $M_B$ ,  $N_H = 1.41$ , and  $N_N = 1$ . All resonating nodes and NRNs are defined at  $\Omega = 0$ .

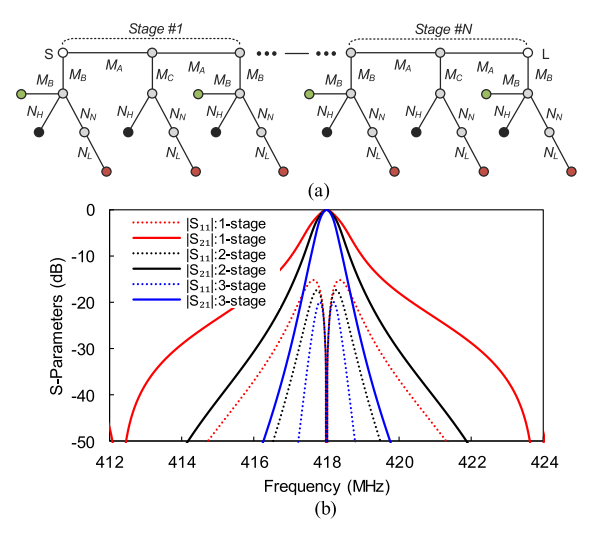


Fig. 3. (a) CRD of an N-stage AWLR-based BPF. (b) Synthesized S-parameters for different number of stages.

TZs as shown in Fig. 2(b). In a practical filter development, their location can be varied by altering the impedance of  $R_L$  in relation to  $R_H$  through  $C_R$  and  $L_R$ .

The selectivity and out-of-band rejection of the AWLR-based symmetrical-quasi-reflectionless BPFs can be increased by cascading in series multiple stages and by merging their interconnecting BSF branches—for size compactness—as shown in the N-stage CRD in Fig. 3(a). In this manner, an N-stage filter comprises N BPF and N+1 BSF sections and its power transmission response is shaped by N poles and 2N TZs. Ideally designed examples are shown in Fig. 3(b). As can be seen, by increasing the number of stages, the out-of-band rejection is increased along with the input—output matching in the passband and stopband regions and the BPF BW decreases.

# III. EXPERIMENTAL VALIDATION

To show the practical viability of the BPF concept, two prototypes were manufactured using commercially available SAW resonators from Abracon Corporation ( $L_M=119.6~\mu{\rm H}$ ,  $C_M=1.511$  fF, series resonance  $\sim\!418$  MHz). They include a tunable-BW single-stage and static two-stage filters on a Rogers 4003 substrate. Fig. 4 shows the prototype of the single-stage along with its component parts.  $M_A$  and  $M_B$  are represented by their  $\pi$ -type low-pass circuit equivalent, whereas  $M_C$  with its corresponding high-pass one. To achieve

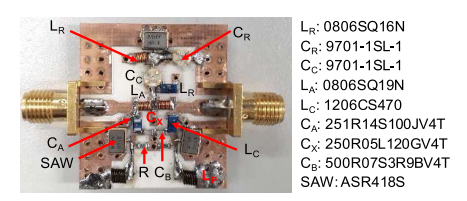


Fig. 4. Manufactured prototype of the single-stage BPF. The admittance inverter  $M_C$  ( $C_C$  and  $L_R$ ) is realized with its  $\pi$ -type high-pass circuit equivalent, whereas  $M_A$  ( $C_X$ ,  $L_A$ , and  $C_A$ ) and  $M_B$  ( $C_B$ ,  $L_C$ , and  $C_A$ ) with their low-pass one.

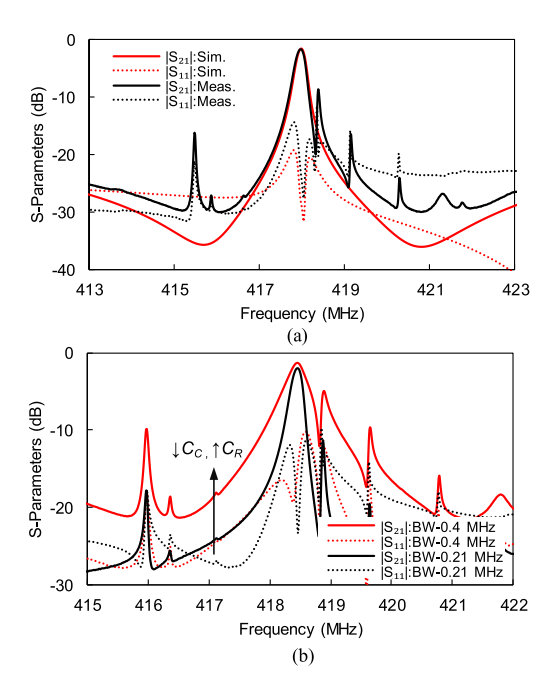


Fig. 5. Measured and simulated S-parameters of the single-stage prototype. (a) Comparison of one simulated and one measured state. (b) RF-measured response of two continuously tunable BW states. Despite only two states are shown, any BW state within 0.21–0.4 MHz can be obtained.

BW tuning, trimmer capacitors (1-5 pF) are incorporated in  $M_C$  and the  $C_R$  element of the AWLR and are tuned asynchronously as shown in Fig. 5. In particular, Fig. 5(a) shows a comparison between one measured and one electromagnetic-(EM)-simulated state-obtained in ADS Keysight in which all AWRs are modeled by their simplified BVD model-which, as can be seen, is in a fairly close agreement. The observed discrepancies are attributed to fabrication and assembly errors. Continuously tunable 3-dB BW between 0.21 and 0.4 MHz (1.9:1 tuning ratio) is proven in Fig. 5(b). Broader BW states can be obtained by decreasing  $C_C$  and increasing  $C_R$ . The performance metrics of the singlestage BPF can be summarized as follows: continuously tunable 3-dB BW in the range of 0.21–0.4 MHz and FBW in the interval of  $0.7-1.3k_t^2$ , minimum in-band insertion loss (IL) < 2 dB- $Q_{\rm eff} > 4500$  and return loss (RL) > 10 dB throughout its entire passband and stopband regions. The measured spurious response is due to the multimode nature of the SAW. They are typically observed in any SAW-based filter as for example in [1], [7], [8]. Alternative methods have been reported for their suppression, including the selective removal of the SiO<sub>2</sub> film from the SAW electrodes [9]. However, such fabricationrelated advancement is out of the scope of this letter, which

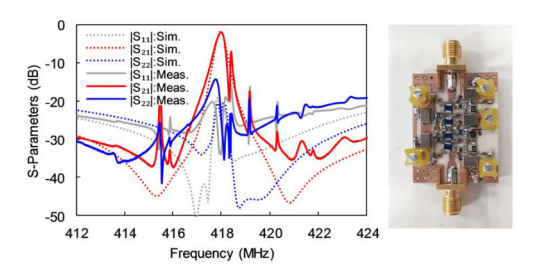


Fig. 6. Two-stage prototype and RF-measured/simulated S-parameters.

aims to demonstrate the design of a new type of tunable-BW quasi-reflectionless SAW BPF.

The measured/simulated S-parameters of the two-stage prototype-  $M_A$ ,  $M_B$ , and  $M_C$  are represented by their low-pass  $\pi$ -type circuit equivalent—are shown in Fig. 6 and are in a fairly close agreement. Its measured metrics are summarized as follows. 3-dB BW of 0.37 MHz, FBW of  $1.2k_t^2$ , minimum in-band IL of 2 dB– $Q_{\rm eff}$  > 6500—and RL >15 dB throughout its entire passband and stopband ranges. As expected, its selectivity is higher than in the one-stage prototype, which validates the scalability of this concept to multistage realizations. As an important advantage to be highlighted in relation to conventional AWR-based filter concepts, the AWLR-based BPF prototypes exhibit FBWs>  $k_t^2$ , hence demonstrating their ability for FBW enhancement.

### IV. CONCLUSION

AWR-based BPFs with symmetrical quasi-reflectionless characteristics have been presented. The proposed concept allows the realization of 1) symmetrical quasi-reflectionless behavior at both of the input and output ports; 2) continuously tunable passband BW in which the quasi-reflectionless behavior is maintained; and 3) enhanced FBW. Two 418-MHz proof-of-concept prototypes were manufactured and tested.

# REFERENCES

- C. C. W. Ruppel, "Acoustic wave filter technology—A review," *IEEE Trans. Ultrason., Ferroelectr., Freq. Control*, vol. 64, no. 9, pp. 1390–1400, Sep. 2017.
- [2] B. Mini-Circuits, "Reflectionless filters improve linearity and dynamic range," *Microw. J.*, vol. 58, no. 8, pp. 42–50, Aug. 2015.
- [3] D. Psychogiou and R. Gómez-García, "Reflectionless adaptive RF filters: Bandpass, bandstop, and cascade designs," *IEEE Trans. Microw. Theory Techn.*, vol. 65, no. 11, pp. 4593–4605, Nov. 2017.
- [4] T.-H. Lee, B. Lee, and J. Lee, "First-order reflectionless lumped-element lowpass filter (LPF) and bandpass filter (BPF) design," in *IEEE MTT-S Int. Microw. Symp. Dig.*, San Francisco, CA, USA, May 2016, pp. 1–4.
- [5] M. A. Morgan and T. A. Boyd, "Theoretical and experimental study of a new class of reflectionless filter," *IEEE Trans. Microw. Theory Techn.*, vol. 59, no. 5, pp. 1214–1221, May 2011.
- [6] M. A. Morgan and T. A. Boyd, "Reflectionless filter structures," *IEEE Trans. Microw. Theory Techn.*, vol. 63, no. 4, pp. 1263–1271, Apr. 2015.
- [7] D. Psychogiou, D. J. Simpson, and R. Gómez-García, "Input-reflection-less acoustic-wave-lumped- element resonator-based bandpass filters," in *IEEE MTT-S Int. Microw. Symp. Dig.*, Philadelphia, PA, USA, Jun. 2018, pp. 852–855.
- [8] D. Psychogiou, R. Gómez-García, and D. Peroulis, "Continuously-tunable-bandwidth acoustic-wave resonator-based bandstop filters and their multi-mode modeling," in *Proc. 46th Eur. Microw. Conf.*, London, U.K., Oct. 2016, pp. 894–897.
- [9] H. Nakamura, H. Nakanishi, R. Goto, and K.-Y. Hashimoto, "Suppression of transverse-mode spurious responses for saw resonators on SiO<sub>2</sub>/Al/LiNbO<sub>3</sub> structure by selective removal of SiO<sub>2</sub>," *IEEE Trans. Ultrason., Ferroelectr., Freq. Control*, vol. 58, no. 10, pp. 2188–2193, Oct. 2011.